Adaptation of microbial resource allocation affects modeled long term soil organic matter and nutrient cycling

Thomas Wutzler[a], Sönke Zaehle[a,b], Marion Schrumpf[a], Bernhard Ahrens[a], Markus Reichstein[a,b]

[a] *Max Planck Institute for Biogeochemistry, Hans-Knöll-Straße 10, 07745 Jena, Germany*
[b] *Michael Stifel Center Jena for Data-driven and Simulation Science, Jena, Germany*

Abstract

In order to understand the coupling of carbon (C) and nitrogen (N) cycles, it is necessary to understand C and N-use efficiencies of microbial soil organic matter (SOM) decomposition. While important controls of those efficiencies by microbial community adaptations have been shown at the scale of a soil pore, an abstract simplified representation of community adaptations is needed at ecosystem scale. Therefore we developed the soil enzyme allocation model (SEAM), which takes a holistic approach to describe C and N dynamics at the spatial scale of an ecosystem and time-scales of years and longer. We explicitly modelled community adaptation strategies of resource allocation to extracellular enzymes and enzyme limitations on SOM decomposition. Using SEAM, we explored whether alternative strategy-hypotheses can have strong effects on SOM and inorganic N cycling. Results from prototypical simulations and a calibration to observations of an intensive pasture site showed that the revenue enzyme allocation strategy was most viable. It accounts for microbial adaptations to both, stoichiometry and amount of different SOM resources, and supported largest microbial biomass under a

wide range of conditions. Predictions of the SEAM model were qualitatively similar to models explicitly representing competing microbial groups. With adaptive enzyme allocation under conditions of high C/N ratio of litter inputs, N was made accessible, which was formerly locked in slowly degrading SOM pools, whereas with high N inputs, N was sequestered in SOM and protected from leaching. The findings imply that it is important for ecosystem scale models to account for adaptation of C and N use efficiencies in order to represent C-N couplings. The combination of stoichiometry and optimality principles is a promising route to yield simple formulations of such adaptations at community level suitable for incorporation into land surface models.

Keywords: soil, enzyme, model, stoichiometry, adaptation, microbe

---

1. Introduction

The global element cycles of carbon (C) and nitrogen (N) are strongly linked and cannot be understood without their intricate interactions (Thornton et al., 2007; Janssens et al., 2010; Zaehle and Dalmonech, 2011). The ties between nutrient cycles are especially strong in the dynamics of soil organic matter (SOM), because the depolymerisation and mineralisation of SOM relies on a microbial community with a rather strict homeostatic regulation of their stoichiometry, i.e. their elemental ratio of C/N (Sterner and Elser, 2002; Zechmeister-Boltenstern et al., 2015).

Decomposers can - in principle - adjust in three different ways when faced with imbalances between the stoichiometry of the organic material (OM), i.e. the litter and SOM they feed on, and their own stoichiometric requirements

(Mooshammer et al., 2014b). First, individual microbes can adapt their carbon-use efficiency (CUE), or their nutrient-use efficiency (NUE) (Sinsabaugh et al., 2013). The alteration of CUE has shown to have large consequences on prediction of carbon sequestration in SOM (Allison, 2014; Wieder et al., 2013). Regulation of nutrient use efficiency has consequences for nutrient recycling and loss of nutrients from the ecosystem (Mooshammer et al., 2014a) and soil plant feedback (Rastetter, 2011). Second, decomposer communities can adapt their stoichiometric requirements. Community composition can shift between species with high C/N ratio, such as many fungi, or species with lower C/N ratio, such as many bacteria (Cleveland and Liptzin, 2007; Xu et al., 2013), although the flexibility is very narrow. Third, decomposers can adapt their allocation of resources into synthesis of different extracellular enzymes to preferentially degrade fractions of SOM that differ by their stoichiometry (Moorhead et al., 2012).

Representation and consequences of stoichiometry on element cycling differ between models at different scales. Most models at ecosystem scale employ the first option, and use changes in CUE or nutrient use efficiency to represent stoichiometric controls on respiration and mineralization fluxes (Manzoni et al., 2008). However, modelling studies at the pore scale have demonstrated the important effect of community adaptation and their emerging effects on element cycling (Allison and Vitousek, 2005; Resat et al., 2011; Wang et al., 2013). Explicite representation of competition among several microbial groups that differ in their expression of different enzymes resulted in a comparable simulated CUE across a wide range of litter stoichiometry (Kaiser et al., 2014). Likely, therefore, there is a need to capture the effects

of community adaptation also in models at ecosystem scale.

At least two alternatives exist to represent the effects of microbial diversity at the ecosystem scale. First, competition of several microbial populations can be explicitly modelled to represent stoichiometric effects such as sustained sequestration of N with high N inputs (Perveen et al., 2014). Second, adaptation of effective properties of the entire microbial community, such as investments into nutrient uptake (Rastetter et al., 1997; Rastetter, 2011), can represent the emerging effects in an abstract, but dynamic and adaptive way. The adaptation of enzyme allocation was recently formalised using the second strategy by the conceptual EEZY model (Moorhead et al., 2012). While this model shows strong strategy effects on nutrient cycling in time scale of days to months, it does not represent feedback mechanisms to the size and stoichiometry of the SOM pools, and therefore cannot study the consequences for decadal SOM dynamics.

In this paper, we adopt the second alternative as working hypothesis and propose a holistic scheme to represent effects of microbial adaptation of enzyme synthesis on SOM cycle at the ecosystem scale. Our aim was to tackle the need of capturing the decadal time scale effects of adaptive enzyme synthesis on SOM dynamics and nutrient recycling. We therefore extended the EEZY model to explore different consequences of alternative enzyme allocation strategies.

This paper first introduces the SEAM model (Section 2.1), a dynamical model of SOM cycling that explicitly represents microbial strategies of producing several extracellular enzyme pools (Section 2.3). Next, the effects of those strategies on SOM cycling are presented by prototypical examples (Sec-

tions 2.4 and 3.1). Finally, a calibration to an intensive pasture site (Section 2.5) demonstrates the usability of the model (Section 3.2) and compares its predictions to the ones of the Symphony model (Perveen et al., 2014), which explicitly models several microbial-groups.

2. Methods

2.1. Soil Enzyme Allocation Model (SEAM)

The dynamic Soil Enzyme Allocation Model (SEAM) allows to explore consequences of enzyme allocation strategies for SOM cycling at the soil core to ecosystem scale. The modelled system are C and N pools in SOM in a representative elemental volume of soil. The system could be soil of a laboratory incubation or a layer of a soil profile, e.g. its upper 20 cm. The model represents different SOM pools containing C and N as state variables and specifies differential equations for the mass fluxes. It is driven by C and N inputs of plant litter (both above-ground and rhizodeposition), inorganic N inputs from deposition and fertilisers, as well as prescribed uptake of inorganic N by roots. SEAM computes output fluxes of heterotrophic respiration and leaching of inorganic N at monthly to decadal time scale.

Key features are: first, the representation of several SOM pools that differ by their stoichiometry, and second, the representation of specific enzymes that degrade those SOM pools. The quality spectrum is modelled by two classes: a C rich litter pool, L, and a N rich pool that consists of microbial residues, R (Fig. 1). The most important assumptions are described in the following paragraphs, while the symbols are explained in Tab. A.5 and detailed model equations are given in Appendix Appendix A.

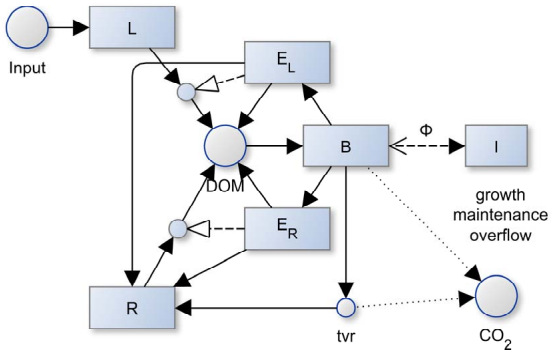

Figure 1: Model structure of SEAM: Two substrate pools (L and R) which differ in their elemental ratios are depolymerized by respective enzymes (E_L and E_R). The simple organic compounds (DOM) are taken up by the microbial community and used for synthesizing new biomass (B), new enzymes, or for catabolic respiration. Stoichiometric imbalance between DOM and B causes overflow respiration or mineralization/immobilization (Φ_B) of inorganic N (I) (further detailed in Fig. 2). Boxes correspond to pools, disks to fluxes, black arrow heads to mass fluxes, white arrow heads to other controls. Solid lines represent fluxes of both C and N, while dotted and dashed lines represent separate C or N fluxes respectively.

Decomposition of the litter and residue pools follows an inverse Michaelis-Menten kinetics (Schimel and Weintraub, 2003), which is first-order to the amount of OM, and saturates with the amount of the respective enzyme. C/N ratios, β, of the decomposition flux are equal to the C/N ratios of the decomposed pool. The C/N ratios of biomass and enzymes are assumed to be fixed, while those of the substrate pools may change over time due to changing C/N ratio of total influxes to these pools. Imbalances in stoichiometry of uptake and microbial requirements are compensated by overflow respiration or N mineralization. Total enzyme allocation is a fixed fraction, a_E, of the microbial biomass, B, per time. However, the microbial community can use different strategies to adjust their allocation to synthesis of alternative kinds of new enzymes (Section 2.3). The DOM pool is assumed to be in

Table 1: State variables and input with initial values and input fluxes. Values refer to the Laqueuille pasture calibration.

Symbol	Definition	Value	Unit	Rational
L	C in litter	571	g m^{-2}	quasi steady state
L_N	N in litter	8.15	g m^{-2}	(Perveen et al., 2014) (by their N/C ratio β)
R	C in residue substrate	10500	g m^{-2}	(Allard et al., 2007) (total stocks - L - dR)
R_N	N in residue substrate	968	g m^{-2}	by C/N ratio in (Perveen et al., 2014)
E_L	C in enzymes targeting L	0.34	g m^{-2}	quasi steady state
E_R	C in enzymes targeting R	0.20	g m^{-2}	quasi steady state
B	microbial biomass C	89.2	g m^{-2}	quasi steady state
I	inorganic N	2.09	g m^{-2}	(Perveen et al., 2014)
input_L	litter C input	969.16	g $m^2 yr^{-1}$	(Perveen et al., 2014) ($m_p C_p^{obs}$)
i_I	inorganic N input	22.91	g $m^2 yr^{-1}$	(Perveen et al., 2014)
k_{IP}	inorganic plant N uptake	16.04	g $m^2 yr^{-1}$	(Perveen et al., 2014) (assuming plant steady state: plant N export + litter N input)

quasi steady state. Hence, the sum of all influxes to the DOM pool, i.e. decomposition plus part of the enzyme turnover, is taken up by the microbial community. If expenses for maintenance and enzyme synthesis cannot be met, the microbial community starves and declines in biomass.

2.2. Exchange with inorganic N pools

The imbalance flux, Φ_B (A.12c), lets microbes mineralise excess N, or immobilise required N up to a maximum rate, $u_{\text{imm,Pot}}$. The latter is assumed to increase linearly with the inorganic N pool. While this stoichiometric imbalance flux is the most widely implemented flux mechanism between mi-

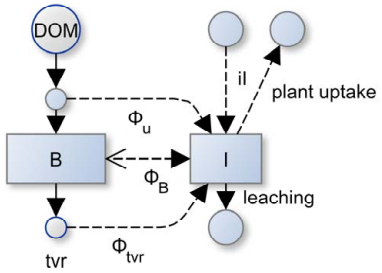

Figure 2: In addition to the maybe negative imbalance flux, Φ_B of microbial biomass, B, there are additional mineralization fluxes feeding the inorganic pool, I, due to mineralization during uptake, Φ_u, and mineralization during microbial turnover, Φ_{tvr}. The N dynamics depends also on fluxes across the system boundary, namely input of organic N with litter, input of inorganic N iI, leaching, and plant uptake of inorganic N.

crobial biomass and the inorganic carbon pool in SOM models (Manzoni and Porporato, 2009), it is not sufficient to recycle N to the inorganic pool if microbial biomass is itself N limited. Therefore, two additional mineralisation fluxes are implemented in SEAM (Fig. 2). First, a fraction of microbial DON uptake, Φ_u (termed uptake mineralisation), is mineralised to represent the subscale imbalance flux at C-limited spots of a heterogeneous soil volume, which is in total not C-limited (Manzoni et al., 2008). Second, a fraction of microbial turnover is mineralised that accounts for grazing. Grazers respire a fraction of the grazed biomass C to meet their energy demand, and - assuming invariant grazer stoichiometry - must release an equivalent amount of nutrients. This mineralization component, here termed turnover mineralization Φ_{tvr}, has been formalised in the soil microbial loop hypothesis (Clarholm, 1985; Raynaud et al., 2006).

In the light of the introduction of these additional N mineralisation fluxes, a refinement of the term N-limitation (Table 2) is required. When microbes cannot meet their stoichiometric demand by DOM uptake but can meet

Table 2: Increasing levels of N limitation

Term	Definition
Organic N lim.	N in microbial uptake of organic matter is less than constrained by other elements ($\Phi_B < 0$).
Microbial N lim.	uptake of organic matter plus maximum immobilisation flux is not enough to satisfy microbial N requirements ($-\Phi_B \geq u_{\mathrm{imm,Pot}}$).
Decomposer system N lim.	There is a net transfer from the inorganic pool to the organic pools ($\Phi = \Phi_B + \Phi_u + \Phi_{\mathrm{tvr}} < 0$).

their demand by immobilising inorganic N, we suggest the term *organic N limitation*. When the immobilisation flux cannot meet the stoichiometric requirement of the microbial community, we suggest the term *microbial N-limitation*. Despite the maximum microbial immobilisation flux there might still be a net mineralization in the system due to uptake mineralization and turnover mineralization. When there is a net N immobilizsation in the system, i.e. a net transfer from the inorganic pool to the organic pools of SOM and microbial biomass, we suggest the term *decomposer system N limitation*. While the two first terms are relevant for microbial ecology, the last term is controlling N availability for plants.

2.3. Enzyme allocation strategies

Microbes allocate a proportion α of their total enzyme investments, $a_e\, B$, to the synthesis of enzymes targeting the N-rich R substrate and a proportion

Table 3: Microbial enzyme allocation strategies

Strategy	Allocation is
Fixed	independent, constant
Match	adjusted to achieve balanced growth, i.e. β_{DOM} matches microbial demands
Revenue	proportional to return per investments into enzymes

$1-\alpha$ to the synthesis of enzymes targeting the N-poor, but better degradable L substrate (1). Three different strategies of allocating investments among synthesis of alternative enzymes were explored in this study (Table 3).

$$\mathrm{syn}_{E_R} / (\mathrm{syn}_{E_R} + \mathrm{syn}_{E_L}) \equiv \alpha \tag{1}$$

The **Fixed** strategy assumes that allocation is independent of, and not changing with changes in substrate availability.

$$\alpha = \text{const.} = 1/2 \tag{2}$$

This strategy corresponds to the models without enzyme allocation adaptation where decomposition rate is a function of microbial biomass (Wutzler and Reichstein, 2008).

The **Match** strategy assumes that microbes regulate enzyme synthesis in a way that the decomposition products balance their stoichiometric demands (Moorhead et al., 2012). The partitioning coefficient α (1) is derived by equating the C/N ratio of the sum of uptake fluxes after other expenses, such as growth and maintenance respiration, to the C/N ratio of microbial

biomass, β_B.

$$\beta_B = \frac{\epsilon(\mathrm{dec}_L + \mathrm{dec}_R - r_M)}{\mathrm{dec}_L / \beta_L + \mathrm{dec}_R / \beta_R - \Phi_M}, \tag{3}$$

where dec_L, and dec_R are depolymerisation fluxes of the litter and residue pools, respectively, which both are a function of α. r_M is maintenance respiration, ϵ is the anabolic microbial efficiency accounting for growth respiration (A.7), β_i are C/N ratios of the respective pools i, and Φ_M is the net flux of N from living microbes to the mineral N pool. Equation 3 for simplicity neglects the small inputs of enzymes to DOM. Here, we assume that microbes use the maximal immobilisation of inorganic N, $u_{\mathrm{imm,Pot}}$ (A.9) to meet their stoichiometric requirements with the Match strategy. Hence, the net N imbalance flux is the difference between mineralization during uptake and the immobilisation: $\Phi_M = \Phi_u - u_{\mathrm{imm,Pot}}$. With microbial N-limitation, (3) has no solution. In this case, the enzyme effort is allocated entirely to the N-rich substrate ($\alpha = 1$), and excess carbon uptake is respired by overflow respiration.

If current enzyme pools E_S, are assumed to be in quasi steady-state with their respective substrate $S \in \{L, R\}$ and microbial biomass, then equation 3 can be solved for partitioning coefficient, α.

$$\alpha_M = f_{\alpha\mathrm{Fix}}(L, \beta_L, R, \beta_R, E_L, E_R, r_M, \Phi_M) \tag{4a}$$

$$\alpha = \begin{cases} 0, & \text{if} \alpha_M \leq 0 \\ 1, & \text{if} \alpha_M \geq 1 \\ \alpha_M, & \text{otherwise} \end{cases} \tag{4b}$$

where the long equation (4a) is given with supplementary material together with R-code and the SYMPY script of its derivation. The bound to one is necessary to handle the case of microbial N-limitation. The bound to zero corresponds to the theoretical case where the C-rich substrate may not suffice to cover microbial C demands relative to N demands.

The **Revenue** strategy assumes that the microbial community adapts in a way to ensure that the investment into enzyme synthesis is proportional to its revenue, i.e. the return per investment regarding the currently limiting element:

$$\alpha_C = \frac{\mathrm{rev}_{RC}}{\mathrm{rev}_{LC} + \mathrm{rev}_{RC}} \tag{5a}$$

$$\alpha_N = \frac{\mathrm{rev}_{RN}}{\mathrm{rev}_{LN} + \mathrm{rev}_{RN}}, \tag{5b}$$

where rev_S is the revenue from given substrate $S \in \{L, R\}$ under C and N-limitation respectively. The return is the current decomposition flux from the substrate degraded by the respective enzyme, and the investment is assumed

to be equal to enzyme turnover to keep current enzyme levels, E_S^*.

$$\mathrm{rev}_{SC} = \frac{\text{return}}{\text{investment}} = \frac{\mathrm{dec}_{S,Pot}\,\frac{E_S^*}{K_{M,S}+E_S^*}}{k_{NS}E_S^*} = \frac{\mathrm{dec}_{S,Pot}}{k_{NS}(K_{M,S}+E_S^*)} \tag{6a}$$

$$\mathrm{rev}_{SN} = \frac{\mathrm{dec}_{S,Pot}\,\frac{E_S^*}{K_{M,S}+E_S^*}/\beta_S}{k_{NS}E_S^*/\beta_E} = \mathrm{rev}_{SC}\,\frac{\beta_E}{\beta_S}, \tag{6b}$$

where k_{NS} is rate of enzyme turnover, $K_{M,S}$ is enzyme's substrate affinity, $\mathrm{dec}_{S,Pot}$ is enzyme saturated decomposition flux (A.4), and β are C/N ratios of the respective pools.

There are two resulting partitioning coefficients, α_C and α_N with C or N-limited microbial biomass, respectively. In order to avoid frequent large jumps under near co-limitation, SEAM implements a smooth transition between these two cases as a weighted average.

$$\alpha = \frac{w_{\mathrm{CLim}}\alpha_C + w_{\mathrm{NLim}}\alpha_N}{w_{\mathrm{CLim}} + w_{\mathrm{NLim}}}, \tag{7}$$

where w is the strength of the limitation of the respective element, specifically the ratio of required to available biomass synthesis fluxes (A.13).

2.4. Prototypical simulation experiments

Several prototypical simulation experiments (Table 4) were used to explore the consequences of the different microbial enzyme allocation strategies (2.3) for the simulated SOM dynamics. They increase in complexity from a soil incubation experiment to a decadal CO_2 manipulation treatment. All experiments used parameter values given in Table A.5 unless stated otherwise. For the prototypical experiments, the inorganic N pool was kept constant at $I = 0.4$ gN m^{-2}, while inorganic N feedbacks were considered in Section 2.5.

Table 4: Prototypical simulation experiments

Experiment	Explored issue
VarN-Incubation	Efficieny of using given fixed substrate levels that vary by N content
Feedback-Steady	Possibility and size of steady state substrate pools
Priming	Increased substrate decomposition and mineralization after a pulse addition of fresh litter
CO_2-Fertilization	Contiued increase of litter C inputs but constant litter N inputs

The **VarN-Incubation** experiment explored to which efficiency substrates of given a stoichiometry are used for microbial biomass growth with the different enzyme allocation strategies. A simplified model version was used in this experiment, where all the inputs and feedback to the substrate pools (L and R) were neglected, and in which these pools were kept constant ($dL/dt = dR/dt = 0$). This simplification led to a quasi steady state of microbial biomass and enzyme levels for the given substrate supply. This experiment mimics a short-term incubation experiment, where changes in litter and residue pools are negligible small. The assumed boundary conditions for this experiment were fixed substrate carbon of $L = 100$ gC m^{-2}, and $R = 400$ gC m^{-2}. The C/N ratio of the residue pool was assumed constant at $\beta_R = 7$, whereas litter C/N ratio varied between 18 and 42 ($\beta_L = [18, .., 42]$).

The **Substrate-feedback** experiment explored the decadal trajectories of the entire system including feedback to the substrate pools. Litter input

was assumed constant at a rate of $\text{input}_L = 400$ gC $\text{m}^{-2}\text{yr}^{-1}$ with a C/N ratio of $\beta_{\text{input}_L} = 30$.

The **Priming** experiment explored the effect of rhizosphere priming, i.e the input of fresh litter into a bulk subsoil. Specifically, the simulations evaluated the fluxes after an addition of 50 g C and a respective amount of N (C/N ratio $\beta_{\text{input}_L} = 30$) on a soil that otherwise received a litter input of only 30 gC $\text{m}^{-2}\text{yr}^{-1}$ (and respective N with $\beta_{\text{input}_L} = 30$) for a decade. The assumption is made that the litter input was very easily degradable litter, specifically with a maximum turnover of $k_L = 10$ day^{-1}.

The CO_2**-Fertilization** experiment explored the effect of continuous litter C input, which is expected with elevated atmospheric CO_2 concentration. The simulations started from steady state corresponding to initial litter C input of $\text{input}_L = 400$ gC $\text{m}^{-2}\text{yr}^{-1}$, applied 20% increased C inputs during years 10 to 60, and applied initial litter inputs again during the next 50 years. The litter N inputs were kept constant over time, implying an increase in the litter C/N ratio of 20%.

2.5. Calibration to a fertilised pasture site

To test the capacity of SEAM to simulate the net carbon storage of a pasture site including feedback of the inorganic N pool, we calibrated the model to data of an intensive pasture. The intensive pasture calibration was tackled only with the Revenue strategy, because the Match strategy had already been proven invalid with the prototypical Feedback experiment and the control case of the Fixed strategy did not allow for adaptation of microbial enzyme allocation.

The model drivers and most of the parametrisation and drivers (Tables

A.5 and 1) were taken from Perveen et al. (2014). The site is a temperate permanent pasture located at an altitude of 1040m a.s.l. in France (Laqueuille, 4538'N, 244'E), receives an annual precipitation of 1200 mm and has an annual mean temperature of 7 C.

The N-balance of the fertilised pasture is characterised by high inorganic N-inputs. A fraction of this N is sequestered in accumulating SOM, a fraction is lost to leaching, while the remainder is exported with plant biomass harvest. Plant uptake of inorganic N was computed as the sum of plant litter production and plant biomass exports, keeping the plant N pool constant.

Model parameters were chosen corresponding to Table 1 in Perveen et al. (2014), and initial litter and SOM pools were prescribed to observed values. Three parameters were calibrated: the maximum decomposition rates of substrate pools, k_L and k_R, and the anabolic carbon-use efficiency, ϵ. Initial pools of microbial biomass and enzymes were set to the decadal steady state in order to prevent large transient initial fluctuations in model pools. The calibration used the *optim* function from R *stats* package (R Core Team, 2016) and minimised the differences between model predictions and observations normalised by the standard deviation of the observations. The calibration used observations of the litter OM, the inorganic N, leaching, and rate of change of the total SOM pool ($\approx dR/dt$ if L is near quasi steady state).

Subsequently, the calibrated parameters were used to generate predictions for several scenarios of altered inputs to the system.

The R-code to generate the results and figures of this paper is available upon request.

3. Results

First, the results of several prototypical artificial simulation experiments clarify the general behaviour and features of the SEAM model. Next, results of a parameter calibration demonstrate the model's ability to simulate the observed C and N dynamics of an intensive pasture and explore feedbacks with the dynamics of the inorganic N pool.

3.1. Prototypical simulation experiments

Under the **VarN-Incubation** experiment, in which the substrate pools were fixed, there were marked differences in the effect of allocation strategies on simulated biomass and the imbalance flux (Fig. 3).

The Match strategy allowed balanced growth, and yielded the highest substrate efficiency and lowest mineralization fluxes among the enzyme allocation strategies. Across a range of litter C/N ratios of 22 to 42 microbes did not need stoichiometric imbalance fluxes, i.e. mineralization of excess N or overflow respiration of excess C. However, it also yielded lowest biomass among the strategies. When the litter contained enough N, microbes invested all resources into litter degrading enzymes. Producing less biomass means to loose competition with other microbes that are able to produce more biomass from given substrates.

With the Revenue strategy, enzyme allocation also varied with litter N content, but to a lesser extent. With litter containing enough N (low C/N ratio), still about 5% of the enzyme synthesis C expenditures were allocated into R degrading enzymes. This resulted in higher mineralization of excess N, but in turn allowed for a higher microbial biomass. With high C/N

ratio of litter, investment into R-degrading enzymes increased to about 30%, much less than with the Match strategy. Hence, the Revenue strategy yielded higher overflow respiration associated with a low carbon-use efficiency (CUE), because of a larger composition flux of the limiting element N.

The Fixed strategy yielded higher N-mineralization due to stoichiometric imbalance at low C/N ratios. At high C/N ratios its constant allocation coefficient was intermediate between the other strategies, leading to intermediate values of all the other outputs.

When the substrate pools were allowed to be refuelled by microbial and enzyme turnover with the **Substrate-feedback** experiment, both Fixed and the Revenue strategies caused substrate pools to approach a steady state. However, the microbes with Match strategy solely degraded the stoichiometrically better matching high-N residue pool, R. Hence, they declined together with the R residues pool despite the large amount of N accumulating in the stoichiometrically less favourable litter pool (Fig. 4). Because of the Match strategy was not able to simulate reasonable stocks when including feedback to substrate pools in the model, it was omitted in the following simulation experiments.

When the soil was amended with a pulse of litter with the **Priming experiment**, a clear true priming effect, i.e. an increased decomposition of the existing SOM, was simulated with the Fixed and Revenue strategy. The priming effect occurred due a strong enhancement of residue decomposition (Fig. 5). This enhancement was stronger with the Revenue strategy than with the Fixed strategy, primarily because of a higher simulated microbial biomass with the Revenue strategy. In consequence, also the N-

mineralization flux due to microbial turnover was larger with the Revenue strategy (Fig. 5). Note, that the time scale of the simulated priming effect of more than 100 days was longer than observed in priming experiments.

When the continuous litter C input was assumed to be higher for 50 years with the CO_2**-fertilisation experiment**, enzyme allocation strategies yielded marked difference in SOM stocks (Fig. 6) and nutrient recycling (Fig. 7). While litter stocks, L, increased with both strategies following the increased input, the residues stock, R, slightly increased with the Fixed strategy, but declined strongly with the Revenue strategy. This was the consequence of an increased mining of the R pool with the Revenue strategy. Accordingly, N mineralization was much stronger with the Revenue strategy during elevated CO_2 period, with largest contribution from mineralization by microbial turnover. In this experiment the microbes were organic N limited ($\Phi_B < 0$), but the decomposer system was not N limited, i.e. there was a total N flux towards the plant accessible inorganic N pool ($\Phi_u + \Phi_B + \Phi_{\text{tvr}} > 0$). The adaptive Revenue strategy helped plants to liberate more N from SOM under elevated CO_2, but this response was transient. After litter inputs returned to initial values, the system recovered towards the initial state but only on centennial time scale that would even be longer if prescribing a longer turnover time for slower SOM pools.

3.2. Intensive pasture simulation

The calibrated SEAM model successfully simulated the observed C and N balance of the Laqueuille intensive pasture (Figure 8). In contrast to the prototypical simulation experiments, here, the feedback of the inorganic N pool was included, the model was driven and compared to observed values,

and only the Revenue strategy has been considered.

The observed continuous build-up of an organic N pool in the residue SOM was driven by the system's positive N balance. Two pathways caused the model behaviour in SEAM. First, inorganic N was taken up by the plant and returned to the soil via organic N in litter. Second, microbial biomass immobilised inorganic N due to its stoichiometric imbalance with the substrate. The microbial biomass was N-limited when only considering uptake of organic substrate. However, it was C-limited when accounting for immobilisation of inorganic N.

Simulated alteration of C and N inputs to the system strongly affected the internal SOM and nutrient cycling. Effects were shown by several simulation scenarios that started from the calibrated state but applied a step change in inputs of litter or inorganic N (Figure 9) as detailed in following paragraphs.

Increased litter C input by 50% together with an increased litter C/N ratio by 25% (elevated CO_2 scenario) caused a shift in enzyme allocation towards enzymes degrading the N-rich residue pool and an increase of the litter pool. The higher input also increased the mineral N demand of both the plant to balance increased biomass synthesis and the microbial biomass with its higher stoichiometric imbalance. The resulting decrease in mineral N also decreased leaching losses. Moreover, ecosystem available N was re-used more often, because of a higher turnover flux of N in increased microbial biomass.

Decreased inorganic N inputs from 22.9 g $m^{-2}yr^{-1}$ down to 1 g $m^{-2}yr^{-1}$ together with a doubling of litter C/N ratio caused a strong shift in enzyme allocation towards enzymes degrading the N-rich residue SOM with similar

consequences as with increased C input, such as an increase in litter OM. However, in this scenario, the decreased N inputs caused a depletion of the mineral N pool. As a consequence, the microbial biomass could not use immobilisation to balance substrate stoichiometry and became N-limited. This caused overflow respiration and a decreasing trend in residue SOM.

Increased inorganic N inputs from 22.9 g $m^{-2}yr^{-1}$ up to 25.6 g $m^{-2}yr^{-1}$ together with a decrease of litter C/N by 25% did not much affect the system behaviour, because the soil system was already C-limited at the start. The microbial biomass could only immobilise a small fraction of the additional N to build up new SOM. Instead, N accumulated in the inorganic pool with associated increased losses to leaching.

4. Discussion

Microbial adaptation of enzyme synthesis to substrate availability benefited the community so that higher microbial biomass levels could be sustained on a wider range of substrate stoichiometry. The different prototypic simulation experiments and the simulation of the intensive pasture led to similar conclusions on the effects of adaptation of enzyme allocation.

4.1. Amounts of substrates matter

The amount of substrate and the substrate stoichiometry are both important for regulating enzyme allocation. The Match strategy failed to account for substrate amount, assuming that microbes can achieve balanced growth under a wide range of substrate stoichiometry (Moorhead et al., 2012; Ballantyne and Billings, 2014). This strategy yielded lower microbial biomass both in the VarN-Incubation (Fig. 3) and in the Substrate-feedback experiments

(Fig. 4). Hence it would be outcompeted by other strategies. Match-strategy microbes focused on degrading a stoichiometrically balanced, but declining residues pool, leaving the large amount of N available in a stoichiometrically less favourable litter pool untouched (Fig. 4). This finding implies that microbial enzyme allocation strategies must account for substrate amounts.

4.2. Community adaptation leads to a more efficient substrate usage

The adaptive Revenue strategy consistently supported higher biomass and had lower N mineralization fluxes at steady state compared to the the non-adaptive Fixed strategy with the VarN-Incubation experiment (Fig. 3). Similar patterns appeared with the other experiments (Figs. 4 and 7). Such better substrate usage is in line with results of individual based small-scale modelling (Kaiser et al., 2014). The finding implies that N mineralization fluxes with imbalanced substrates may be lower than inferred from previous modelling studies that did not account for community adaptation.

4.3. Comparison to observed changes in enzyme stoichiometry

The SEAM model focuses on community adaptation of enzyme synthesis. It predicts a change in the ratio of enzyme activities of enzymes degrading C-rich plant litter versus enzymes degrading the N-rich residue SOM when changing inputs of inorganic N to the soil. While only low variation in stoichiometry of N-degrading versus C-degrading enzymatic activity is observed across biomes (Sinsabaugh et al., 2009), microcosm studies detect short-term changes of enzyme activities with N fertilization (Kumar et al., 2016), but their observations differ between different kinds of N-degrading enzymes. Hence, the evidence is mixed.

SEAM also predicts accelerated turnover of the residue pool associated with increased enzyme activity of N-degrading enzymes after increased inputs of litter C in relation to litter N. Such patterns are observed at field scale at Duke forest, where Phillips et al. (2011) found an increased activity of extracellular enzymes involved in breakdown of organic N associated with accelerated SOM turnover after increased root exudation with elevated CO_2. In an artificial root exudation experiments at the same site, Drake et al. (2013) found an increase of N degrading NAG enzyme activity with C-only inputs and a shift from oxidative towards hydrolytic enzymes decomposing low molecular weight (lmw) components with C+N inputs. Assuming that the lmw-components have higher C/N ratios, this observed shift is in line with SEAM predictions.

4.4. SOM as nutrient bank

Nitrogen was stored in residue SOM during periods of high N inputs and released during periods of low N inputs relative to C inputs in simulations (Fig. 6). When there was excess litter carbon, the microbial community preferentially depolymerised, or mined, the N-rich residue pool, and thereby made the N available for plants. When carbon inputs were low, microbes degraded the residue pool to a lesser extent, but continued to build new residue via microbial turnover. Hence, under low C conditions, the microbes kept N in the decomposer system instead of releasing it through mineralisation.

This 'bank' mechanism (sensu Perveen et al., 2014) also worked when simulating the intensive pasture (Fig. 9). During simulations of high inorganic N inputs, N was sequestered in SOM at a high rate. With decreased inorganic N inputs, the sequestration rate decreased until it became negative,

that is the N in slower decomposing SOM pools was mined. In the long-term, i.e. centuries, the inputs to the system have to balance the outputs of the system. Hence, in the intensive pasture simulation, inorganic N pools and N leaching increased with the increase of SOM with the SEAM model. The conservation or release of N by the bank mechanism implies greater potential for ecosystems to avoid progressive N limitation (Norby et al., 2010; Franklin et al., 2014; Averill et al., 2015). This finding potentially has consequences on feedbacks of global change, especially on the projected C land uptake (Friedlingstein et al., 2014).

4.5. Priming effects liberate N

Priming effects, i.e. the altered decomposition of SOM after soil amendments (Kuzyakov et al., 2000), are a potential mechanism to help plants stimulate N release from the SOM for plant nutrition. Priming effects and associated increased N mineralization were simulated for both, the Fixed and Revenue strategies (Fig. 5). With adaptive microbial enzyme allocation (Revenue strategy), increasing plant litter input or increases in litter C/N upregulated the decomposition of the N-rich residue pool (Fig. 6). This in turn influenced the distribution of N in the ecosystem, and N availability for plants (Fig. 7). This active role of plant inputs has been demonstrated in a soil incubation experiment (Fontaine et al., 2011) and has been further conceptualised with the SYMPHONY model (Perveen et al., 2014). Our results are in line with these studies, although our explanation is on a more abstract level (see Section 4.7).

Mineralization during microbial turnover is important for nutrient recycling. Without the additional mineralization mechanisms of uptake mineral-

ization (Manzoni et al., 2008) and turnover mineralization (Clarholm, 1985; Raynaud et al., 2006) in our simulation experiment, microbes shifted enzyme allocation to degrade the residues pool, but the N was then sequestered in microbial biomass and not mineralised to inorganic N. Hence, our simulation experiments reinforced the need for representing soil heterogeneity and microbial turnover by grazing for making N available for plants under N limitation.

4.6. Mismatch in time scale of priming effects

The unrealistically long time-scale of the priming effect of several months in SEAM (Fig. 5) resulted from both, the long turnover time of enzymes, and the sustaining positive feedback between amounts of microbial biomass and enzymes. It was in contrast with incubation studies that observe priming effects within days or weeks that rapidly declined after the amendment has been used up (Blagodatskaya et al., 2014). The priming timescale in SEAM was longer than the duration of the uptake pulse of the L amendment that only lasted a few days. It was controlled by simulated lifetime of enzymes and enzyme turnover, which SEAM described as first order kinetics with a turnover of about a week. Moreover, the priming timescale was prolonged by the positive feedback of increased microbial biomass producing more enzymes that again fuelled microbial biomass.

One possible cause for a shorter priming time-scale is a different dynamics of enzyme turnover. However, prescribing a shorter turnover time of enzymes would require an unrealistically large effort of producing enzymes by microbial biomass. More sophisticated models of different enzyme turnover kinetics including stabilisation of a part of the enzymes on mineral surfaces

(Burns et al., 2013) may be able to resolve such contradictions. Testing this hypothesis would require observations of the fraction of C uptake allocated to enzyme synthesis and on age distribution of enzymes in the soil which might be feasable with labelling studies.

An alternative cause for a shorter priming time-scale may be an important control of enzyme activity that is not strongly coupled to microbial biomass dynamics. Some enzymes such as peroxidase need to be fuelled by labile OM themselves (Rousk et al., 2014) with no immediate relationship to microbial biomass dynamics. This explanation, however, implies that enzyme activity and decomposition of SOM become largely decoupled from enzyme synthesis and microbial dynamics in the short-term. This option is contrary to the assumption of most current models that simulate the priming effect. Such a fundamental change of model assumption would affect most implications gained from SOM modelling studies that involve soil microbes.

Another cause for a shorter priming time-scale, is a diminished sustaining positive feedback between enzymes and microbial biomass. Currently, grazing is modelled as an implicit part of a first-order microbial turnover. With increasing microbial biomass, grazers become more efficient (Clarholm, 1981). With implementing a time-lagged stronger increase in microbial turnover rate with microbial biomass, biomass levels would decrease faster to pre-treatment levels and help to shorten the time-scale of the priming effect. Testing this hypothesis requires data on grazing during priming effects.

Overall, the mismatch in the time scale of priming between simulations and observations hints to gaps in understanding of short-term SOM turnover. However, this model limitation does not impair the simulated longer-term

microbial community controls on SOM cycling both in the prototypic simulation and at the pasture site. We argue therefore that the simulated decadal patterns are robust, because they are more strongly controlled by the proportions in enzyme synthesis than by the time scale of priming effects.

4.7. A holistic view for upscaling

The presented SEAM model takes a holistic view (Panikov, 2010) of microbial community and their adaptations instead of explicitly describing microbial diversity. In this respect, it differs from the SYMPHONY model (Perveen et al., 2014) and similar models (Fontaine et al., 2003), which explicitly model several microbial groups. However, the effective behaviour of the presented SEAM model is similar to these models. SEAM assumes that community composition is to a large extent driven by external drivers. Specifically, SEAM describes an adaptive allocation of resources into breakdown of different substrates by assuming that the community composition adapts to changed substrate availability in a way to balance microbe's revenue of the currently limiting element. While the mechanistic approach of the SYMPHONY model explicitly represents this adaptation by shifts between microbial groups, the holistic approach represents its effects at community level. While the mechanistic approach provides more detailed understanding, the proposed abstraction of microbial competition is a step forward to better represent couplings of soil carbon and nutrient cycles in large-scale ecosystem models, as it obviates the need to correctly parameterise the underlying mechanisms.

The holistic SEAM model yielded qualitatively similar predictions as the mechanistic SYMPHONY model with simulating priming, the bank mecha-

nism, and a continuous SOM sequestration under high inorganic N inputs. SEAM differed from SYMPHONY in the prediction of the inorganic N pool during low N inputs. Specifically, SEAM predicted a decrease in this pool, while SYMPHONY predicted an increase in this pool due to changed competition (Perveen et al., 2014). The difference is probably caused by different assumptions on how the DOM pool is shared among groups of the microbial community and resulting different competition conditions. In SEAM, decomposition products become mixed in a shared DOM pool, while in the SYMPHONY model the decomposition products are not shared between the microbial groups. The truth at pore scale is in between, in that decomposition products are mainly used by the group that is producing the extracellular enzymes, while a part of the DOM diffuses also to other groups (Kaiser et al., 2014). At larger scales, such details cannot be measured or resolved. The difference in model prediction implies that the rationality of the simplified model assumptions of a mixed DOM pool can be qualitatively tested against observations.

4.8. Testable predictions of change of SOM C/N ratios

The SEAM model can be used to predict decadal patterns of SOM cycling following changes in substrate stoichiometry. Observations of such patterns provide evidence for or against the modelling assumptions. Specifically, SEAM predicted a change in proportions of the litter pool and the SOM pool (Fig. 6). While these abstract pools are not directly comparable to observations, a measurable consequence is the associated change of total SOM C/N ratio at the time scale of turnover of the residue pool. Specifically, SEAM predicted a decline in SOM stocks and an increase of SOM C/N with

FACE experiments at formerly C-limited systems over time scales of several decades. Observed accelerated SOM turnover at the Duke forst after 12 years of elevated CO_2 (Drake et al., 2011) is a first indications, although there ist a continuum of responses to experimental CO_2 increase across sites.

4.9. Outlook

The biggest limitation of the SEAM model is its focus on a single process: community adaptation of enzyme allocation. In order to focus, we had to ignore several other important processes. One such process is the second microbial community strategy of handling substrate stoichiometric imbalance, the adaption of stoichiometry of microbial biomass. Although the potential of this biomass adaptation is thought to be quite limited (Mooshammer et al., 2014b), it will need to be tested whether these two strategies can be combined within a model.

Next, the optimality principle will be extended to also determine the proportion of uptake that is allocated to enzyme synthesis. Presence of cheaters, i.e. microbes that consume substrate but without producing enzymes, effectively lower the community-level allocation to enzymes (Kaiser et al., 2014). Community development can be assumed to maximise biomass production. Such an assumption can be used to compute the optimal community enzyme synthesis and allows exploring effects on SOM cycling, such as more constrained carbon and nutrient use efficiencies.

Moreover, SEAM will be simplified by assuming quasi-steady state of biomass or enzyme pools (Wutzler and Reichstein, 2013). These simplifications will lead to fewer parameters and improved parameter identifiably in model calibration to observations. Together with implementing the influ-

ence of environmental factors such as temperature and moisture (Davidson et al., 2012), these changes will make SEAM more suitable to be used as a component within larger scale land surface models.

5. Conclusions

The SEAM model (Fig. 1) provides a holistic description of community adaptations. It yields qualitatively similar predictions as microbial-group-explicit models with the ability to represent priming effects, bank mechanism, and a continuous SOM sequestration with high inorganic N inputs (Fig. 9). Hence, this study provides an important step for providing an abstract description of microbial community effects and adaptations, with the long-term goal of including the important mechanisms into earth system models.

Adapting the allocation of resources into the synthesis of different enzymes can be an effective means of the microbial community to react to changing substrate stoichiometry. Allocation adaptation strategies helped the simulated microbial biomass in SEAM to grow larger across a wider range of substrate stoichiometry (Fig. 3). Among the tested strategies, the Revenue strategy, which accounts for the amount of substrate pools and their stoichiometry, was particularly successful. These findings imply that models simulating soil carbon and nutrients dynamics (Fig 5) need to account for adaptations in carbon and nutrient strategies. Accounting for adaptations will be especially important when studying the competition for nutrients between soil microorganism and plants, because SOM can function as a storage to sequester surplus nutrients and prevent them from being lost from the system (Fig. 6 and 7).

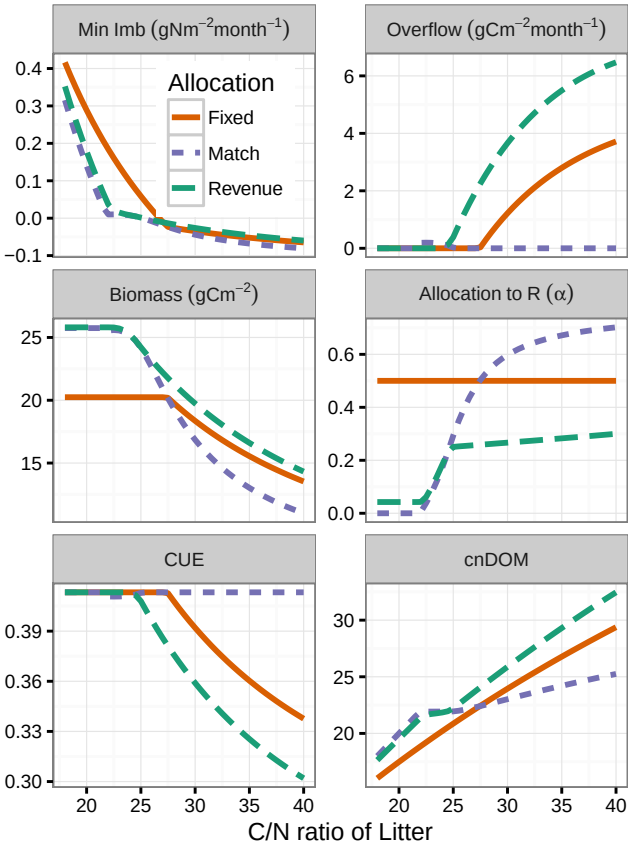

Figure 3: Match enzyme allocations strategy yielded highest resource efficiency, i.e. lowest mineralization fluxes (N mineralization and C overflow respiration) at steady state with the VarN-experiment. Microbes with alternative strategies, however, were more competitive as indicated by a higher biomass. The patterns are caused by different adatption of resource allocation (α) affecting C/N ratio of the decomposition flux (cnDOM) and carbon use efficiency (CUE).

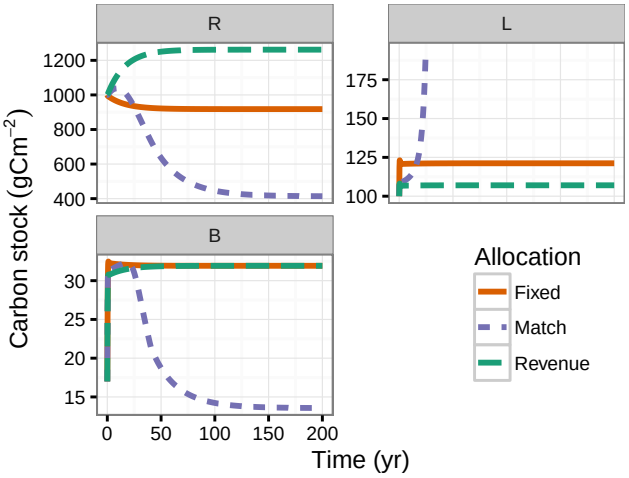

Figure 4: Match strategy was not viable when considering feedback to substrate pools with the SimSteady experiment. Microbes with Match-strategy degraded the stoichiometrically matching but declining R substrate pool and their biomass, B, declined despite the N stores in stoichiometrically less favourable litter, L.

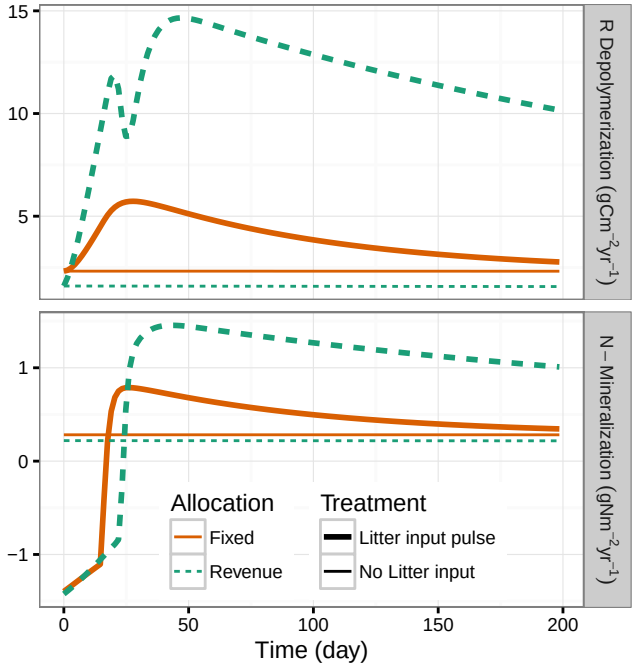

Figure 5: Both depolymerisation of the residue substrate pool and N mineralization were stimulated most strongly with the Revenue strategy after a subsoil has been amended with a pulse of fresh litter (Priming experiment) compared to a control with no amendment (thin horizontal lines).

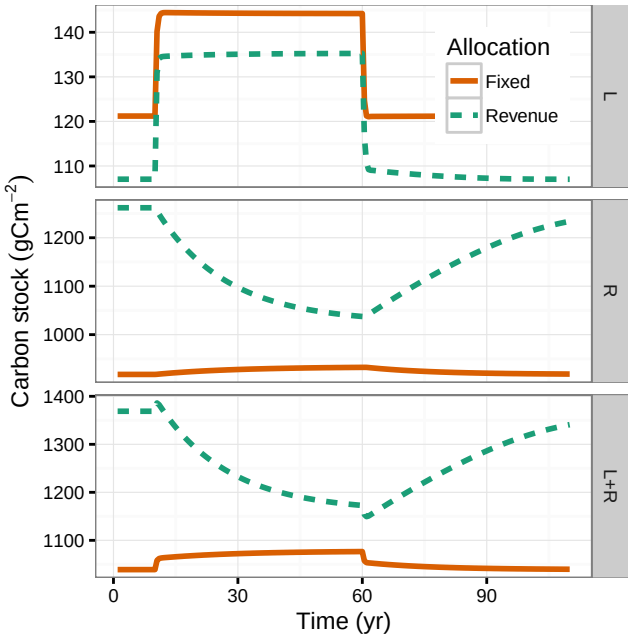

Figure 6: Revenue strategy led to a mining, i.e. decrease, of the residue substrate pool, R, that was stronger than the increase in litter substrate pool, L, during increased carbon litter inputs in years 10 to 60 with the CO_2-Fertilization experiment.

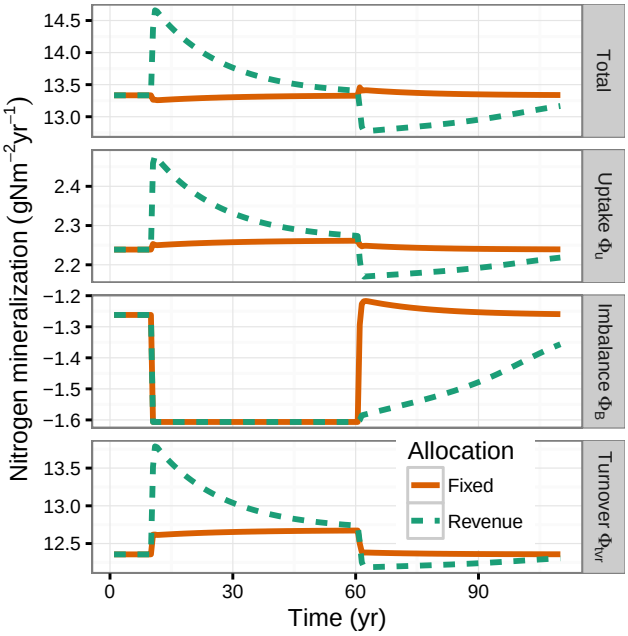

Figure 7: Mineralization of N associated with microbial turnover contributed most of the liberation of SOM-N with the Revenue strategy during CO_2-Fertilisation, which started at year 10. After the end of the fertilisation at year 60, microbies with the Revenue strategy continued to more strongly immobilize N (negative flux Φ_b).

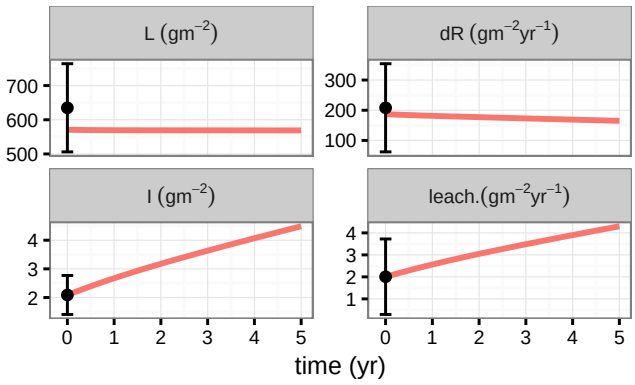

Figure 8: Calibrated SEAM predictions (lines) matched observations from the Laqueuille intensive pasture site (dots and errorbars) of litter pool, L, change of SOM pools, dR, inorganic N, I, and N leaching rate.

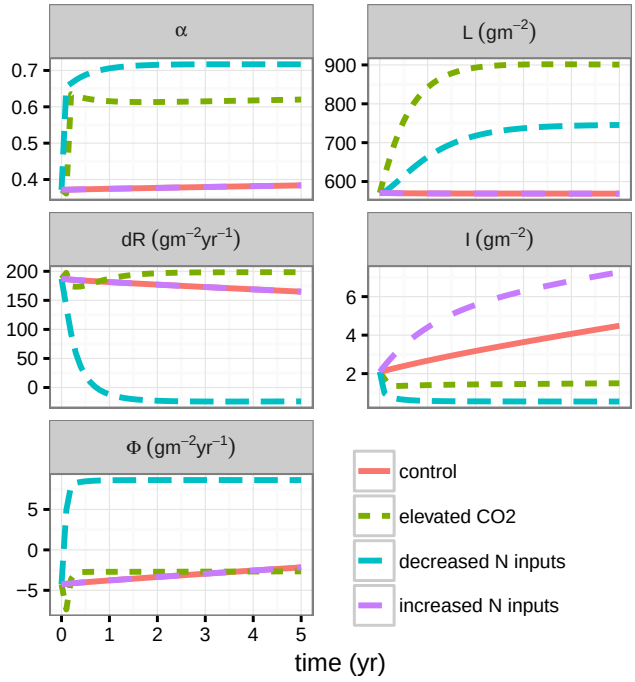

Figure 9: Prescribed alteration of C and N inputs led to subsequent shifts in enzyme allocation (α) and affected development of soil pools. Increased N substrate limitation, either due to elevated CO_2 or due to decreasing inorganic N inputs, caused an increase in litter pool, L, and a decrease in mineral N pool, I. If the substrate N limitation could not be balanced by inorganic N input, then the change rate of the residue pool, dR, decreased down to negative values, i.e. decreasing SOM pools, and a positive N flux, Φ, from SOM to the inorganic N pool.

Appendix A. SEAM equations

For an overview of symbol defintions see tables 1, A.5, and A.6.

Appendix A.1. Carbon fluxes

$$\frac{dB}{dt} = \mathrm{syn}_B - \mathrm{tvr}_B \tag{A.1a}$$

$$\frac{dE_L}{dt} = (1-\alpha)\ \mathrm{syn}_E - \mathrm{tvr}_{EL} \tag{A.1b}$$

$$\frac{dE_R}{dt} = \alpha\ \mathrm{syn}_E - \mathrm{tvr}_{ER} \tag{A.1c}$$

$$\frac{dL}{dt} = -\,\mathrm{dec}_L + \mathrm{input}_L \tag{A.1d}$$

$$\frac{dR}{dt} = -\,\mathrm{dec}_R + \epsilon_{\mathrm{tvr}}\,\mathrm{tvr}_B + (1-\kappa_E)(\mathrm{tvr}_{ER} + \mathrm{tvr}_{EL}), \tag{A.1e}$$

where α is the proportion of total investment into enzymes that is allocated to the residue pool R (section 2.3, input_L is the litter C input to the system, ϵ_{tvr}) is the fraction of microbial turnover C that is respired by predators, and κ_E is the fraction of enzyme turnover that is transferred to the DOM instead of the R pool. The specific fluxes are detailed below.

Total enzyme production syn_E, maintenance respiration r_M, and microbial turnover tvr_B are modelled as a first-order kinetics of biomass:

$$\mathrm{syn}_E = a_E B \tag{A.2a}$$

$$\mathrm{r}_M = mB \tag{A.2b}$$

$$\mathrm{tvr}_B = \tau B \tag{A.2c}$$

606 Enzyme turnover (tvr_{ER} and tvr_{EL}) is modelled as first-order kinetics of
607 enzyme levels.

$$\mathrm{tvr}_{E_S} = k_E E_S, \tag{A.3}$$

608 where S represents the litter L and residue R substrate pools, respectively.

Substrate depolymerisation is modelled first-order to substrate availability with a saturating Michaelis-Menten kinetics to enzyme levels:

$$\mathrm{dec}_{S,Pot} = k_S S \tag{A.4a}$$

$$\mathrm{dec}_S = dec_{S,Pot} \frac{E_S}{K_{M,S} + E_S} \tag{A.4b}$$

609 The DOM pool is assumed to be in quasi steady state, and hence, the
610 sum of all influxes to the DOM pool (decomposition + part of the enzyme
611 turnover) is taken up by microbial community.

$$u_C = \mathrm{dec}_L + \mathrm{dec}_R + \kappa_E(\mathrm{tvr}_{ER} + \mathrm{tvr}_{EL}) \tag{A.5}$$

612 Under C limitation, C available for synthesis of new biomass and associ-
613 ated catabolic growth respiration, C_{synBC}, is the difference between C uptake
614 and expenses for enzyme synthesis (eq. A.2a) and maintenance respiration
615 (eq. A.2b).

$$C_{\mathrm{synBC}} = u_C - \mathrm{syn}_E / \epsilon - \mathrm{r}_M \tag{A.6}$$

616 If the C balance for biomass synthesis, syn_B (eq. A.11), is positive, only
617 a fraction ϵ, the anabolic carbon use efficiency (CUE) is used for synthesis
618 of biomass and enzymes, whereas the rest is used for catabolic growth res-

piration r_G to support this synthesis. The model assumes that requirements for enzyme synthesis and maintenance must be met. Hence, the microbial C balance can become negative where microbial biomass starves and declines.

$$\mathrm{syn}_B = \begin{cases} \epsilon\, C_{\mathrm{synB}}, & \text{if } C_{\mathrm{synB}} > 0 \\ C_{\mathrm{synB}}, & \text{otherwise} \end{cases} \tag{A.7a}$$

$$\mathrm{r}_G = \begin{cases} (1-\epsilon)\, C_{\mathrm{synB}}, & \text{if } C_{\mathrm{synB}} > 0 \\ 0, & \text{otherwise ,} \end{cases} \tag{A.7b}$$

where C_{synB} is the C balance for biomass synthesis and is given below by eq. A.11.

Appendix A.2. Nitrogen fluxes

Nitrogen fluxes and pools are derived by dividing the respective fluxes with the C/N ratio, β, of their source.

The C/N ratios β_B and β_E of the microbial biomass and enzymes are assumed to be fixed. However, the C/N ratio of the substrate pools may

change over time and thus the substrate N pools are modelled explicitly.

$$\frac{dL_N}{dt} = -\operatorname{dec}_L / \beta_L + \operatorname{input}_L / \beta_{\mathrm{i}} \tag{A.8a}$$

$$\frac{dR_N}{dt} = -\operatorname{dec}_R / \beta_R + \epsilon_{\mathrm{tvr}} \operatorname{tvr}_B / \beta_B + (1 - \kappa_E)(\operatorname{tvr}_{ER} + \operatorname{tvr}_{EL}) / \beta_E \tag{A.8b}$$

$$\frac{dI}{dt} = +i_I - k_{IP} - lI + \Phi \tag{A.8c}$$

$$\Phi = \Phi_u + \Phi_B + \Phi_{\mathrm{tvr}} \tag{A.8d}$$

$$\Phi_u = (1 - \nu) u_{N,OM}, \tag{A.8e}$$

where the balance of the inorganic N pool I sums inorganic inputs i_I, plant uptake k_{IP}, leaching lI, and the exchange flux with soil microbial biomass, Φ. The latter is the sum of the apparent mineralization due to soil heterogeneity (Manzoni et al., 2008), Φ_u, mineralisation-immobilisation imbalance flux, Φ_B (A.12c), and mineralisation of a part of microbial turnover ,Φ_{tvr} (A.14b, section Appendix A.5).

Organic N uptake, $u_{N,OM}$, was modelled as a parallel scheme (PAR), where a part of the organic N that is taken up from DON is mineralised accounting at soil core scale accounting for imbalance flux at sub-scale soil spots with high N concentration in DOM (Manzoni et al., 2008). Potential N uptake is the sum of organic N uptake and the potential immobilisation flux ($u_{\mathrm{imm,Pot}}$). Uptake from DOM is assumed equal to influxes to DOM times

the apparent N use efficiency ν.

$$u_N = \nu u_{N,OM} + u_{\text{imm,Pot}} \tag{A.9a}$$

$$u_{N,OM} = \text{dec}_L\,/\beta_L + \text{dec}_R\,/\beta_R + \kappa_E(\text{tvr}_{ER} + \text{tvr}_{EL})/\beta_E \tag{A.9b}$$

$$u_{\text{imm,Pot}} = i_B I, \tag{A.9c}$$

where C/N ratios β_L and β_R are calculated based on current C and N substrate pools: $\beta_L = L/L_N$.

The N available for biomass synthesis is the difference of microbial N uptake and expenses for enzyme synthesis. This translates to a N constraint for the C used for biomass synthesis and its associated catabolic growth respiration: $C_{\text{synB}} \leq C_{\text{synBN}}$.

$$N_{\text{synBN}} = u_N - \text{syn}_E\,/\beta_E, \tag{A.10a}$$

$$C_{\text{synBN}} = \beta_B\, N_{\text{synBN}}/\epsilon \tag{A.10b}$$

Appendix A.3. Imbalance fluxes of C versus N limited microbes

There are constraints of each element on the synthesis of new biomass and associated growth respiration. The minimum of these fluxes (eq. A.11) constrains the synthesis of new biomass.

$$C_{\text{synB}} = min(C_{\text{synBC}}, C_{\text{synBN}}) \tag{A.11}$$

The excess elements are lost by imbalance fluxes (eq. A.12). The excess C is respired by overflow respiration, r_O, and the excess N is mineralised,

M_{Imb}, so that the mass balance is closed.

$$r_O = u_C - (\mathrm{syn}_B + \mathrm{syn}_E / \epsilon + \mathrm{r}_G + r_M) \tag{A.12a}$$

$$M_{\mathrm{Imb}} = u_N - (\mathrm{syn}_B / \beta_B + \mathrm{syn}_E / \beta_E) \tag{A.12b}$$

$$\Phi_B = M_{\mathrm{Imb}} - u_{\mathrm{imm,Pot}} \tag{A.12c}$$

The actual mineralisation-immobilisation flux Φ_B is the difference between the potential immobilisation flux and excess N mineralization. If microbes are limited by C availability, Φ_B will be positive, whereas with substrate N limitation, Φ_B will be a negative flux, corresponding to N immobilisation. With microbial N limitation, i.e. required immobilisation is larger than potential immobilisation, $\Phi_B = -u_{\mathrm{imm,Pot}}$ and stoichiometry must be balanced by overflow respiration.

Appendix A.4. Weight of an element limitation

The weight of an element limitation is computed as the ratio between required uptake flux for given other constraints to the available fluxes for biosynthesis.

$$w_{\mathrm{CLim}} = \left(\frac{\mathrm{required}}{\mathrm{available}} \right)^{\delta} = \left(\frac{C_{\mathrm{synBN}}}{C_{\mathrm{synBC}}} \right)^{\delta} \tag{A.13a}$$

$$w_{\mathrm{NLim}} = \left(\frac{\epsilon \, C_{\mathrm{synBC}} / \beta_B}{N_{\mathrm{synBN}}} \right)^{\delta}, \tag{A.13b}$$

where parameter δ, arbitrarily set to 200, controls the steepness of the transition between the two limitations. X_{synBY} denotes the available flux of element

X for biosynthesis and associated respiration given the limitation of element Y (A.6) and (A.10).

Appendix A.5. Turnover mineralization fluxes

In addition to mineralization flux due to stoichiometric imbalance, a part of microbial biomass is mineralised during microbial turnover, e.g. by grazing. A part $(1 - \epsilon_{\mathrm{tvr}})$ of the biomass is used for catabolic respiration. With assuming that predator biomass elemental ratios do not differ very much from the one of microbial biomass, a respective proportion of N must be mineralized.

$$r_{\mathrm{tvr}} = (1 - \epsilon_{\mathrm{tvr}})\ \mathrm{tvr}_B \tag{A.14a}$$

$$\Phi_{\mathrm{tvr}} = (1 - \epsilon_{\mathrm{tvr}})\ \mathrm{tvr}_B\, / \beta_B \tag{A.14b}$$

All the non-respired turnover C enters the residue pool. In reality, a part of the microbial turnover probably enters the DOM pool again (e.g. by cell lysis) and is taken up again by microbial biomass. The increased uptake nearly cancels with an increased turnover. Hence, SEAM does not explicitly consider this shortcut loop so that fewer model parameters are required. Note, however, that turnover, uptake, and CUE in the model are slightly lower than in the real system where this shortcut operates.

Table A.5: Model parameters. The two value columns of initial values and parameter values refer to the prototypical examples and the Laqueuille pasture calibration respectively.

Symbol	Definition	Value	Value	Unit	Rational
β_B	C/N ratio of microbial biomass	11	11	g g^{-1}	(Perveen et al., 2014)
β_E	C/N ratio of extracellular enzymes	3.1	3.1	g g^{-1}	(Sterner and Elser, 2002)
β_{input_L}	C/N ratio of plant litter inputs	30	70	g g^{-1}	(Perveen et al., 2014) ($1/\beta$)
k_R	maximum decomposition rate of R	1	4.39e-2	yr^{-1}	calibrated
k_L	maximum decomposition rate of L	5	1.95	yr^{-1}	calibrated
k_E	enzyme turnover rate	60	60	yr^{-1}	(Burns et al., 2013)
κ_E	fraction enzyme tvr. entering DOM instead R	0.8	0.8	(-)	mostly small proteins
a_E	enzyme production per microbial biomass	0.365	0.365	yr^{-1}	$\approx 6\%$ of biomass synthesis
K_M	enzyme half saturation constant	0.05	0.05	g m^{-2}	magnitude of DOC concentration
τ	microbial biomass turnover rate	6.17	6.17	yr^{-1}	(Perveen et al., 2014) (s/ϵ_{tvr})
m	specific rate of maintenance respiration	1.825	0	yr^{-1}	(van Bodegom, 2007), zero in (Perveen et al., 2014)
ϵ	anabolic microbial C substrate efficiency	0.5	0.53	(-)	calibrated
ν	aggregated microbial organic N use efficiency	0.7	0.9	(-)	(Manzoni et al., 2008)
ϵ_{tvr}	microbial turnover that is not mineralized	0.3	0.8	(-)	part of turnover is consumed by predators
i_B	maximum microbial uptake rate of inorganic N	25	25	yr^{-1}	larger than simulated immobilization flux
l	inorganic N leaching rate	-	0.959	yr^{-1}	(Perveen et al., 2014) (l)

Table A.6: Further symbols of quantities derived within the system

Symbol	Definition	Unit
α	proportion of enzyme investments allocated to production of E_R	(-)
syn_B	C for microbial biomass synthesis	g m^2yr^{-1}
syn_{E_S}	C synthesis of enzymes degrading $S \in \{L, R\}$	g m^2yr^{-1}
tvr_B	microbial biomass turnover C	g m^2yr^{-1}
tvr_{E_S}	enzyme turnover C	g m^2yr^{-1}
dec_S	C in decomposition of resource $S \in \{L, R\}$	g m^2yr^{-1}
u_C, u_N	microbial uptake of C and N	g m^2yr^{-1}
$\Phi_u, \Phi_B, \Phi_{\text{tvr}}$	N mineralization with microbial DOM uptake, stoichiometric imbalance, and turnover (Fig. 2)	g m^2yr^{-1}

We thank Nazia Perveen and Sébastien Fontaine for letting us reuse the data that they used for fitting the SYMPHONY model. TW acknowleges support from Deutsche Forschungsgemeinschaft CRC 1076 "AquaDiva". SZ acknowledges support from the European Research Council (ERC) under the European Union's Horizon 2020 research and innovation programme (QUINCY; grant no. 647204).

References

Allard, V., Soussana, J.-F., Falcimagne, R., Berbigier, P., Bonnefond, J., Ceschia, E., D'hour, P., Hénault, C., Laville, P., Martin, C., Pinarès-Patino, C., 2007. The role of grazing management for the net biome productivity and greenhouse gas budget (co2, {N2O} and ch4) of semi-natural grassland. Agriculture, Ecosystems & Environment 121, 47 – 58.

Allison, S. D., Oct 2014. Modeling adaptation of carbon use efficiency in microbial communities. Frontiers in Microbiology 5.

Allison, S. D., Vitousek, P. M., May 2005. Responses of extracellular enzymes to simple and complex nutrient inputs. Soil Biology & Biochemistry 37 (5), 937–944.

Averill, C., Rousk, J., Hawkes, C., Nov 2015. Microbial-mediated redistribution of ecosystem nitrogen cycling can delay progressive nitrogen limitation. Biogeochemistry 126, 11–23.

Ballantyne, F., Billings, S., May 2014. Shifting resource availability, plastic allocation to exoenzymes and the consequences for heterotrophic soil respiration. In: EGU General Assembly Conference Abstracts. Vol. 16 of EGU

685 General Assembly Conference Abstracts. p. 16780.
686 URL http://adsabs.harvard.edu/abs/2014EGUGA..1616780B

687 Blagodatskaya, E., Khomyakov, N., Myachina, O., Bogomolova, I., Blago-
688 datsky, S., Kuzyakov, Y., Jul 2014. Microbial interactions affect sources of
689 priming induced by cellulose. Soil Biology and Biochemistry 74, 39–49.

690 Burns, R. G., DeForest, J. L., Marxsen, J., Sinsabaugh, R. L., Stromberger,
691 M. E., Wallenstein, M. D., Weintraub, M. N., Zoppini, A., 2013. Soil
692 enzymes in a changing environment: Current knowledge and future direc-
693 tions. Soil Biology and Biochemistry 58, 216 – 234.

694 Clarholm, M., Dec 1981. Protozoan grazing of bacteria in soil - impact and
695 importance. Microbial Ecology 7, 343–350.

696 Clarholm, M., 1985. Interactions of bacteria, protozoa and plants leading
697 to mineralization of soil nitrogen. Soil Biology and Biochemistry 17 (2),
698 181–187.

699 Cleveland, C. C., Liptzin, D., Aug 2007. C:n:p stoichiometry in soil: is there a
700 redfield ratio for the microbial biomass? Biogeochemistry 85 (3), 235–252.

701 Davidson, E. A., Samanta, S., Caramori, S. S., Savage, K., 2012. The dual
702 arrhenius and michaelismenten kinetics model for decomposition of soil
703 organic matter at hourly to seasonal time scales. Global Change Biology
704 18 (1), 371–384.

705 Drake, J. E., Darby, B. A., Giasson, M.-A., Kramer, M. A., Phillips, R. P.,
706 Finzi, A. C., 2013. Stoichiometry constrains microbial response to root

exudation- insights from a model and a field experiment in a temperate forest. Biogeosciences 10 (2), 821838.

Drake, J. E., Gallet-Budynek, A., Hofmockel, K. S., Bernhardt, E. S., Billings, S. A., Jackson, R. B., Johnsen, K. S., Lichter, J., McCarthy, H. R., McCormack, M. L., Moore, D. J. P., Oren, R., Palmroth, S., Phillips, R. P., Pippen, J. S., Pritchard, S. G., Treseder, K. K., Schlesinger, W. H., DeLucia, E. H., Finzi, A. C., 2011. Increases in the flux of carbon belowground stimulate nitrogen uptake and sustain the long-term enhancement of forest productivity under elevated CO2. Ecology Letters 14 (4), 349357.

Fontaine, S., Henault, C., Aamor, A., Bdioui, N., Bloor, J., Maire, V., Mary, B., Revaillot, S., Maron, P., Jan 2011. Fungi mediate long term sequestration of carbon and nitrogen in soil through their priming effect. Soil Biology and Biochemistry 43 (1), 86–96.

Fontaine, S., Mariotti, A., Abbadie, L., Jun 2003. The priming effect of organic matter: a question of microbial competition? Soil Biology & Biochemistry 35 (6), 837–843.

Franklin, O., Näsholm, T., Högberg, P., Högberg, M. N., May 2014. Forests trapped in nitrogen limitation - an ecological market perspective on ectomycorrhizal symbiosis. New Phytol 203 (2), 657–666.

Friedlingstein, P., Meinshausen, M., Arora, V. K., Jones, C. D., Anav, A., Liddicoat, S. K., Knutti, R., 2014. Uncertainties in cmip5 climate projections due to carbon cycle feedbacks. Journal of Climate 27 (2), 511–526.

729 Janssens, I. A., Dieleman, W., Luyssaert, S., Subke, J.-A., Reichstein, M.,
730 Ceulemans, R., Ciais, P., Dolman, A. J., Grace, J., Matteucci, G., et al.,
731 Apr 2010. Reduction of forest soil respiration in response to nitrogen de-
732 position. Nature Geosci 3 (5), 315–322.

733 Kaiser, C., Franklin, O., Dieckmann, U., Richter, A., Mar 2014. Microbial
734 community dynamics alleviate stoichiometric constraints during litter de-
735 cay. Ecol Lett 17 (6), 680–690.

736 Kumar, A., Kuzyakov, Y., Pausch, J., Jun 2016. Maize rhizosphere priming:
737 field estimates using 13C natural abundance. Plant and Soil.

738 Kuzyakov, Y., Friedel, J. K., Stahr, K., Oct 2000. Review of mechanisms and
739 quantification of priming effects. Soil Biology & Biochemistry 32 (11-12),
740 1485–1498.

741 Manzoni, S., Porporato, A., 2009. Soil carbon and nitrogen mineraliza-
742 tion: Theory and models across scales. Soil Biology and Biochemistry 41,
743 13551379.

744 Manzoni, S., Porporato, A., Schimel, J. P., May 2008. Soil heterogeneity in
745 lumped mineralization-immobilization models. Soil Biology & Biochem-
746 istry 40 (5), 1137–1148.

747 Moorhead, D. L., Lashermes, G., Sinsabaugh, R. L., 2012. A theoretical
748 model of c-and n-acquiring exoenzyme activities, which balances microbial
749 demands during decomposition. Soil Biology and Biochemistry 53, 133–
750 141.

Mooshammer, M., Wanek, W., Hämmerle, I., Fuchslueger, L., Hofhansl, F., Knoltsch, A., Schnecker, J., Takriti, M., Watzka, M., Wild, B., et al., Apr 2014a. Adjustment of microbial nitrogen use efficiency to carbon:nitrogen imbalances regulates soil nitrogen cycling. Nat Comms 5.

Mooshammer, M., Wanek, W., Zechmeister-Boltenstern, S., Richter, A., 2014b. Stoichiometric imbalances between terrestrial decomposer communities and their resources: mechanisms and implications of microbial adaptations to their resources. Frontiers in Microbiology 5.

Norby, R. J., Warren, J. M., Iversen, C. M., Medlyn, B. E., McMurtrie, R. E., Sep. 2010. CO2 enhancement of forest productivity constrained by limited nitrogen availability. Proceedings of the National Academy of Sciences 107 (45), 19368–19373.

Panikov, N. S., 2010. Microbial ecology. Environmental Biotechnology, 121–191.

Perveen, N., Barot, S., Alvarez, G., Klumpp, K., Martin, R., Rapaport, A., Herfurth, D., Louault, F., Fontaine, S., Apr 2014. Priming effect and microbial diversity in ecosystem functioning and response to global change: a modeling approach using the symphony model. Glob Change Biol 20 (4), 1174 – 1190.

Phillips, R. P., Finzi, A. C., Bernhardt, E. S., 2011. Enhanced root exudation induces microbial feedbacks to n cycling in a pine forest under long-term CO2 fumigation. Ecology Letters 14 (2), 187194.

R Core Team, 2016. R: A Language and Environment for Statistical Computing. R Foundation for Statistical Computing, Vienna, Austria.
URL https://www.R-project.org

Rastetter, E. B., Feb 2011. Modeling coupled biogeochemical cycles. Frontiers in Ecology and the Environment 9 (1), 68 – 73.

Rastetter, E. B., Ågren, G. I., Shaver, G. R., May 1997. RESPONSES OF n-LIMITED ECOSYSTEMS TO INCREASED CO2: a BALANCED-NUTRITION, COUPLED-ELEMENT-CYCLES MODEL. Ecological Applications 7 (2), 444–460.

Raynaud, X., Lata, J. C., Leadley, P. W., Sep 2006. Soil microbial loop and nutrient uptake by plants: a test using a coupled c : N model of plant-microbial interactions. Plant and Soil 287 (1-2), 95–116.

Resat, H., Bailey, V., McCue, L. A., Konopka, A., Dec 2011. Modeling microbial dynamics in heterogeneous environments: Growth on soil carbon sources. Microbial Ecology 63 (4), 883–897.

Rousk, J., Hill, P. W., Jones, D. L., Dec 2014. Priming of the decomposition of ageing soil organic matter: concentration dependence and microbial control. Functional Ecology 29 (2), 285–296.

Schimel, J. P., Weintraub, M. N., 2003. The implications of exoenzyme activity on microbial carbon and nitrogen limitation in soil: a theoretical model. Soil Biology and Biochemistry 35, 549–563.

Sinsabaugh, R. L., Hill, B. H., Follstad Shah, J. J., Dec 2009. Ecoenzymatic

795 stoichiometry of microbial organic nutrient acquisition in soil and sediment.
796 Nature 462 (7274), 795–798.

797 Sinsabaugh, R. L., Manzoni, S., Moorhead, D. L., Richter, A., Jul 2013. Car-
798 bon use efficiency of microbial communities: stoichiometry, methodology
799 and modelling. Ecology Letters 16 (7), 930–939.

800 Sterner, R. W., Elser, J. J., 2002. Ecological stoichiometry: the biology of
801 elements from molecules to the biosphere. Princeton University Press.

802 Thornton, P. E., Lamarque, J.-F., Rosenbloom, N. A., Mahowald, N. M., Dec
803 2007. Influence of carbon-nitrogen cycle coupling on land model response
804 to co 2 fertilization and climate variability. Global Biogeochemical Cycles
805 21 (4).

806 van Bodegom, P., May 2007. Microbial maintenance: A critical review on its
807 quantification. Microbial Ecology 53 (4), 513–523.

808 Wang, G., Post, W. M., Mayes, M. A., Jan 2013. Development of microbial-
809 enzyme-mediated decomposition model parameters through steady-state
810 and dynamic analyses. Ecological Applications 23 (1), 255–272.

811 Wieder, W. R., Bonan, G. B., Allison, S. D., Jul 2013. Global soil carbon
812 projections are improved by modelling microbial processes. Nature Climate
813 Change.

814 Wutzler, T., Reichstein, M., 2008. Colimitation of decomposition by sub-
815 strate and decomposers - a comparison of model formulations. Biogeo-
816 sciences 5 (3), 749–759.

817 Wutzler, T., Reichstein, M., Mar. 2013. Priming and substrate quality inter-
818 actions in soil organic matter models. Biogeosciences 10 (3), 2089–2103.

819 Xu, X., Thornton, P. E., Post, W. M., Jun 2013. A global analysis of soil mi-
820 crobial biomass carbon, nitrogen and phosphorus in terrestrial ecosystems.
821 Global Ecology and Biogeography 22 (6), 737–749.

822 Zaehle, S., Dalmonech, D., Oct. 2011. Carbon-nitrogen interactions on land
823 at global scales: current understanding in modelling climate biosphere
824 feedbacks. Current Opinion in Environmental Sustainability 3 (5), 311–
825 320.

826 Zechmeister-Boltenstern, S., Keiblinger, K. M., Mooshammer, M., Penuelas,
827 J., Richter, A., Sardans, J., Wanek, W., May 2015. The application of
828 ecological stoichiometry to plant - microbial - soil organic matter transfor-
829 mations. Ecological Monographs 85 (2), 133–155.